1

Supplementary information

Multi-emission processes of hierarchically structured NaGdF$_4$:Tm:Yb:Tb core@shell nanoparticles.

Amanda Justino de Morais,[a] Airton Germano Bispo-Jr,[a] Flavia de Sousa Ferreira,[a] Italo Odone Mazali,[a] and Fernando Aparecido Sigoli[a]*

[a] Department of Inorganic Chemistry, Institute of Chemistry, University of Campinas, UNICAMP, Campinas, 13083-970, Brazil.

E-mail: fsigoli@unicamp.br

Contents

Supplementary note S1 – Synthesis and characterization

EXPERIMENTAL

Materials and preparation

Ytterbium oxide (Yb_2O_3, 99.9%), yttrium oxide (Y_2O_3, 99.99%), thulium oxide (Tm_2O_3, 99.9%), gadolinium oxide (Gd_2O_3, 99.9%), terbium oxide (Tb_4O_7, 99.95%), trifluoroacetic acid (CF_3COOH, > 99%), oleic acid ($C_{18}H_{34}O_2$, OA, 90%), 1-octadecene ($C_{18}H_{36}$, ODE, 90%), and oleylamine (OM, 70%) were purchased from *Sigma-Aldrich*. Sodium hydroxide (NaOH, > 98%), hydrochloric acid (HCl, 36.5- 38 %), hydrogen peroxide (H_2O_2, 29%), ethanol (C_2H_5OH, 99.5 %), and cyclohexane (C_6H_{12}, 99%) were purchased from *Synth*. All chemicals were used without any further purification.

Lanthanide trifluoroacetates, $[Ln(CF_3COO)_3]$, were prepared by dissolving the lanthanide oxide into a solution containing excessive trifluoroacetic acid and water (90 °C). The resulting solution was slowly evaporated (100 °C) to obtain $[Ln(CF_3COO)_3]$ powders. $[Tb(CF_3COO)_3]$ was prepared by adding stoichiometric amounts of HCl and H_2O_2 in Tb_4O_7 followed by stirring (90 °C) up a transparent solution was formed, which was slowly evaporated and the $TbCl_3$ product was used to get $[Tb(CF_3COO)_3]$ following the previously mentioned procedure. Finally, $Na(CF_3COO)$ was obtained from sodium hydroxide in distilled water after the addition of trifluoracetic acid up to pH = 7. Then, water was evaporated to obtain the solid precursor.

Synthesis of β-NaGdF₄ core@shell and β-NaGdF₄ core@shell@shell nanoparticles

All nanoparticles were synthesized by the decomposition method adapted by Sigoli's group.[1,2,3,4] This method is reproducible,[1,2,3,4] enabling the control of the nanoparticle shape and size, while the crystalline phase can be changed by increasing the temperature from 310 °C (α-phase) to 330 °C (β-phase). OA (15 mmol), ODE (30 mmol), OM (15 mmol), $Na(CF_3COO)$ (1.5 mmol), and $[Ln(CF_3COO)_3]$ (1.5 mmol) were mixed in a round-bottom flask under vacuum at 100 °C (30 min). The temperature was then increased to 310 °C upon Ar atmosphere (15 min) to get the α-NaLnF₄ phase, and after that, the temperature was increased to 330 °C to get the β-NaLnF₄ phase. In the sequence, OA (20 mmol), ODE (20 mmol) and $Na(CF_3COO)$ (2.6 mmol) previously kept at 100 °C were added and the mixture was left to react for 30 min. The

temperature was decreased to 260 °C and [Ln(CF$_3$COO)$_3$] (0.5 mmol total, depending on the doping and composition), Na(CF$_3$COO) (0.5 mmol), OA (10 mmol), ODE (10 mmol), both previously kept at 100 °C, were added in the reactional flask whereas the mixture was stirred for 30 min to let the shell layer to growth. After the process, the system was brought to room temperature. The nanoparticles were precipitated from ethanol, separated by centrifugation (Damon IEC division EG Model K, 3000 rpm, 30 minutes), washed repeatedly with ethanol, cyclohexane/ethanol (1:4 v/v), distilled water/ethanol (1:4 v/v), and finally oven dried (TECNAL - TE39312, 100 °C).

Sample characterization

Powder X-ray diffraction (298 K) was measured in a Shimadzu (XRD 7000) diffractometer by using CuK$_\alpha$ (λ= 1.5418 Å) radiation and scanning speed of 2 ° min^{-1}. Transmission electron microscopy (TEM) images were obtained in a Libra 120 Carl Zeiss microscope, accelerating voltage of 120 kV, and LaB$_6$ thermionic emission. Samples were prepared by dropping 6 µL of a nanoparticle suspension in hexane in a Cu grade with a thin carbon layer (TedPella – LC400-CU-CC-25). The determination of particle size and shell thickness were done in the ImageJ software by considering 400 particles for the average particle size and the shell thicknesses were determined on nanoparticles that we could detect clear differences between core and shell layers. Excitation and emission spectra of powder or cyclohexane suspensions (30 mg mL^{-1}) at 298 K were measured in a Fluorolog-3 (Horiba Jobin-Yvon FL3-22-iHR320) spectrofluorometer while a 980 nm (Crystalaser DL980-1W-T0) or a 488 nm laser (Sapphire 488-75 SF CDRH) with optical power density (P_{exc}) within 2.8 - 61.5 W cm^{-2} were used as excitation source for the emission spectra acquisition. A Xe (*Ozone free*, 450 W) continuous bulb was also used as light source for the excitation spectra acquisition of the core@shell@shell compositions. All spectra were corrected accordingly to the optical system, lamp intensity, and the photomultiplier sensitivity (Hamamatsu R928P and Hamamatsu H10330-75). To avoid second-order harmonic coming from the excitation sources, two filters in the optical path (Edge, 514 nm, and Semrock RazorEdge Dichroic, 488 nm) were kept after the light emission by the sample. Finally, for the calculation of the integrated area in the QC spectra shown in Figure 6d, only the spectral region

from 995 nm to 1060 nm was considered to avoid any contribution of a possible second-order harmonic peak at 976 nm from the excitation laser.
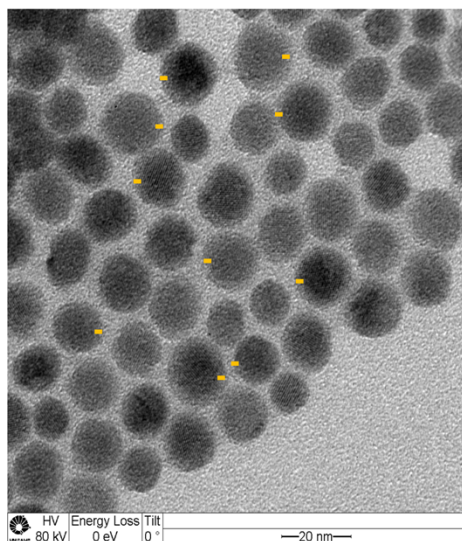
Supplementary note S2 – Additional TEM images of the core@shell nanoparticles
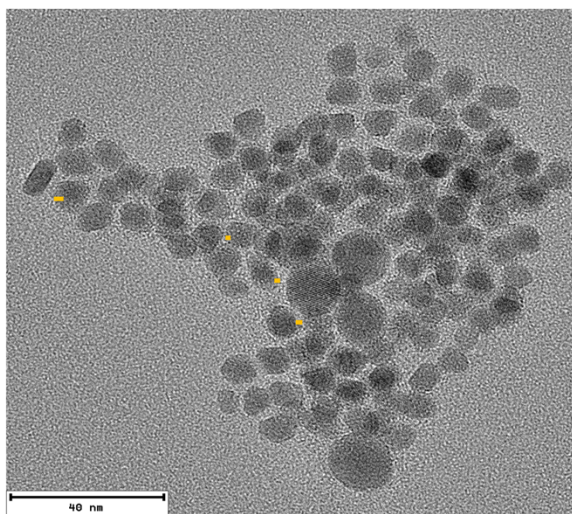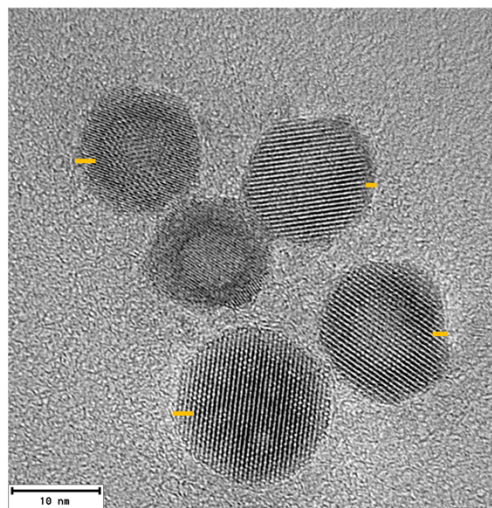
β - NaGd$_{0.765}$Tm$_{0.015}$Yb$_{0.20}$Tb$_{0.02}$F$_4$@NaYF$_4$

β- NaGd$_{0.98}$Tb$_{0.02}$F$_4$@NaGd$_{0.785}$Tm$_{0.015}$Yb$_{0.20}$F$_4$@NaYF$_4$

β- NaGd$_{0.85}$Tb$_{0.15}$F$_4$@NaGd$_{0.785}$Tm$_{0.015}$Yb$_{0.20}$@NaYF$_4$

Figure S1. TEM images of β - NaGd$_{0.765}$Tm$_{0.015}$Yb$_{0.20}$Tb$_{0.02}$F$_4$@NaYF$_4$, β- NaGd$_{0.98}$Tb$_{0.02}$F$_4$@NaGd$_{0.785}$Tm$_{0.015}$Yb$_{0.20}$F$_4$@NaYF$_4$, and β- NaGd$_{0.85}$Tb$_{0.15}$F$_4$@NaGd$_{0.785}$Tm$_{0.015}$Yb$_{0.20}$@NaYF$_4$ compositions, representing also some regions used to determine the shell thicknesses.

Supplementary note S3 – UC features of core@shell nanoparticles
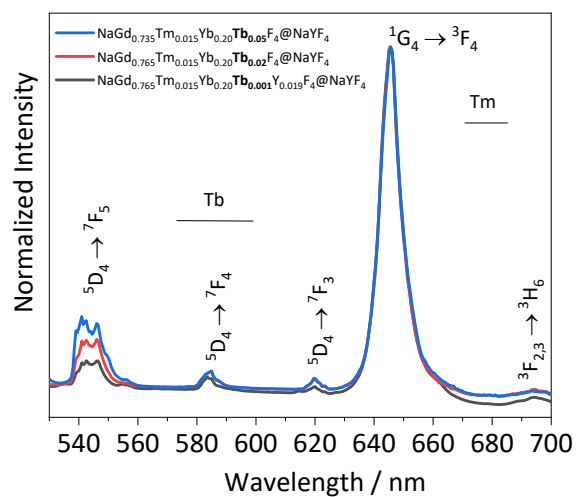
Figure S2. Upconversion spectra (298 K, 980 nm excitation, P_{exc} = 37.3 W cm^{-2}) of β-NaGd$_{y-x}$Tm$_{0.015}$Yb$_{0.20}$**Tb$_x$**F$_4$@NaYF$_4$ nanoparticles with different Tb^{III} doping concentration, x = 0.001 (0.1 mol%), 0.02 (2 mol%), or 0.05 (5 mol%).
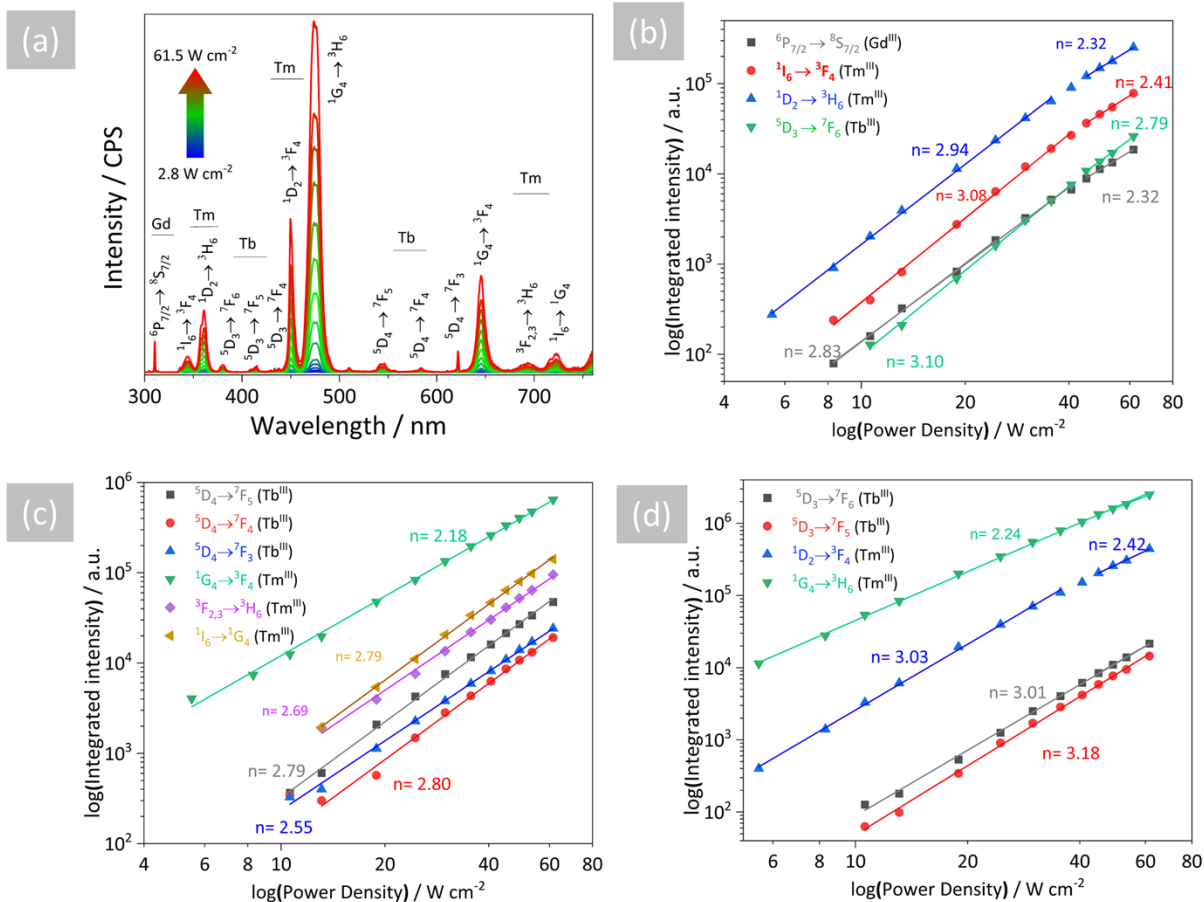
Figure S3. (a) Upconversion spectra of β-NaGd$_{0.765}$Tm$_{0.015}$Yb$_{0.20}$**Tb$_{0.001}$**Y$_{0.019}$F$_4$@NaYF$_4$ (0.1 mol% Tb, powder, 298 K) at P_{exc} ranging from 2.8 to 61.5 W cm^{-2} under 980 nm excitation. Dependence of integrated emission intensities on P_{exc} considering (b) 300 to 400 nm, (c) 400 to 500 nm, and (d) 500 to 760 nm spectral regions.
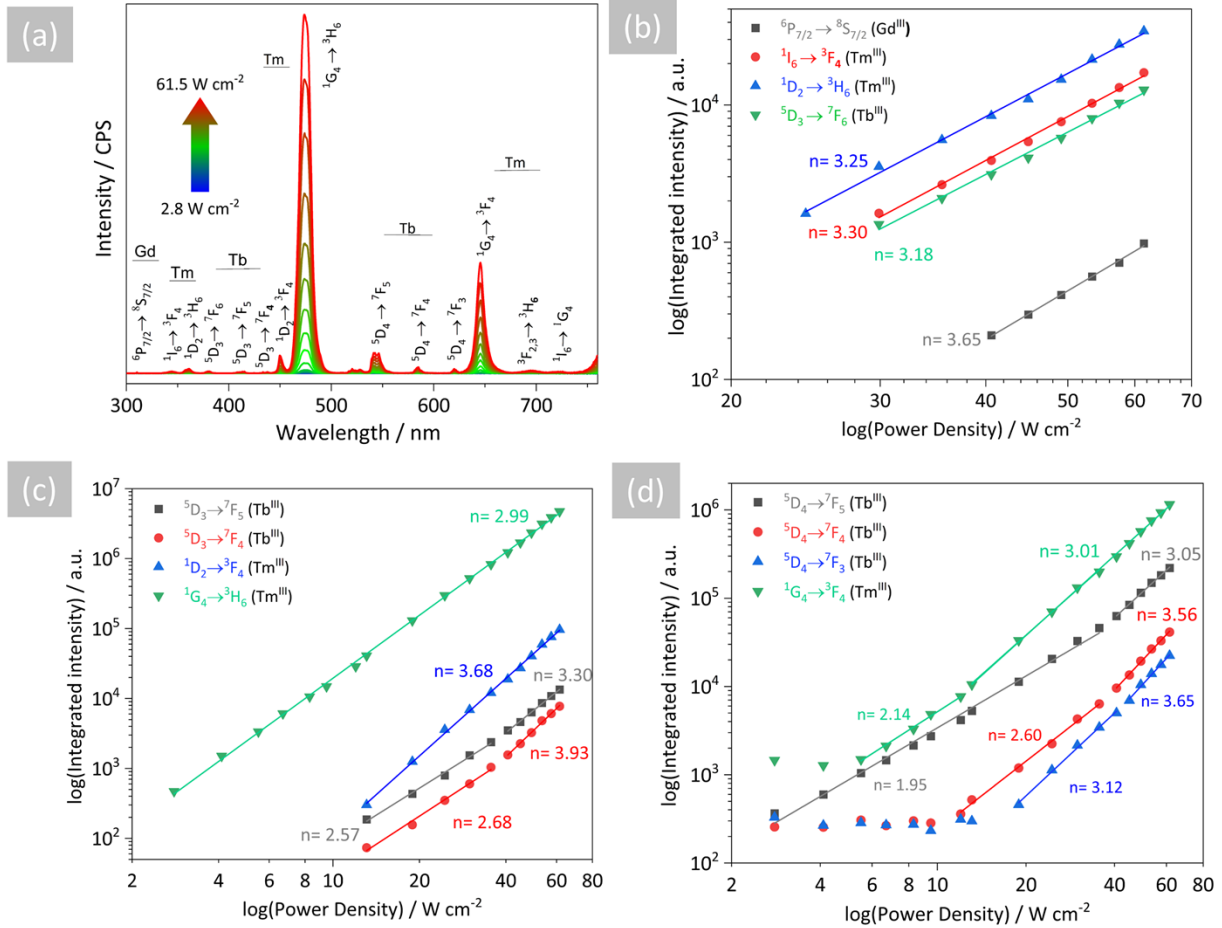
Figure S4. (a) Upconversion spectra of β-$NaGd_{0.735}Tm_{0.015}Yb_{0.20}\mathbf{Tb_{0.05}}F_4@NaYF_4$ (5 mol%Tb, powder, 298 K) at P_{exc} ranging from 2.8 to 61.5 W cm^{-2} under 980 nm excitation. Dependence of integrated emission intensities on the P_{exc} considering (b) 300 to 400 nm, (c) 400 to 500 nm, and (d) 500 to 760 nm spectral regions.

**Supplementary note S4 – Structural characterization of core@shell@shell nanoparticles**
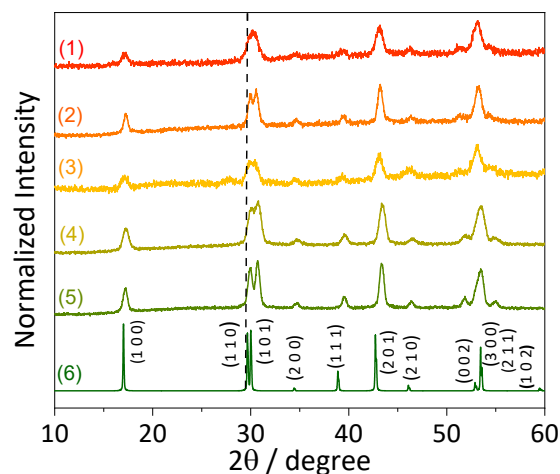
Figure S5. (a) Powder XRD diffraction of (1) β-NaGd$_{0.80}$**Tb$_{0.20}$**F$_4$@NaGd$_{0.785}$Tm$_{0.015}$Yb$_{0.20}$F$_4$@NaYF$_4$, (2) β-NaGd$_{0.85}$**Tb$_{0.15}$**F$_4$@NaGd$_{0.785}$Tm$_{0.015}$Yb$_{0.20}$F$_4$@NaYF$_4$ (3) β-NaGd$_{0.98}$**Tb$_{0.02}$**F$_4$@NaGd$_{0.785}$Tm$_{0.015}$Yb$_{0.20}$F$_4$@NaYF$_4$, (4) β-NaGd$_{0.735}$**Tb$_{0.05}$**Tm$_{0.015}$Yb$_{0.20}$F$_4$@NaYF$_4$, and (5) NaGd$_{0.765}$Tm$_{0.015}$Yb$_{0.20}$**Tb$_{0.001}$**Y$_{0.019}$F$_4$@NaYF$_4$ compared to the (6) β-NaGdF$_4$ standard (JCPDS-PDF: 27-6990).
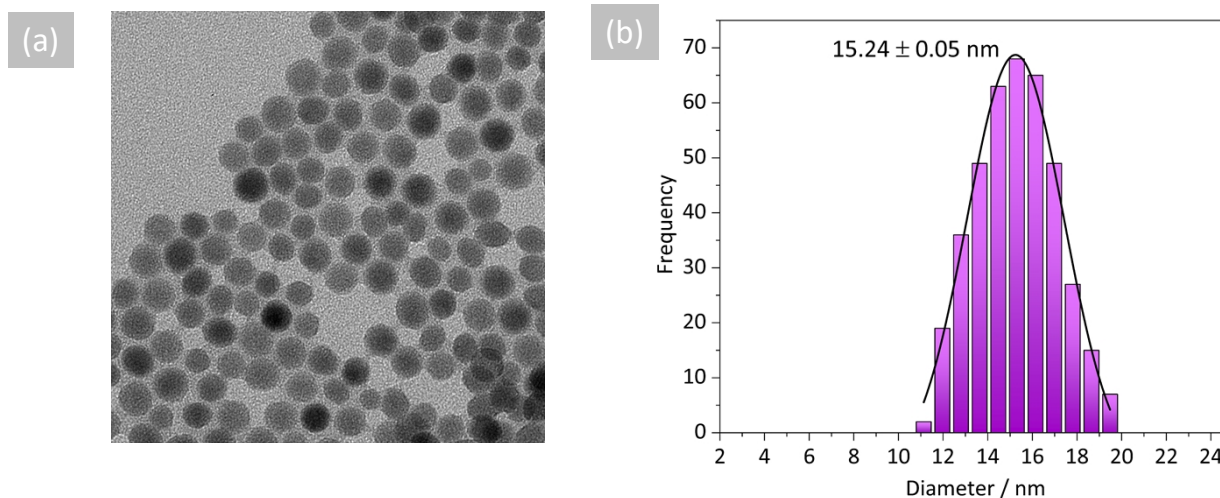
Figure S6. TEM images, and the corresponding size distributions of β-NaGd$_{0.85}$**Tb$_{0.15}$**F$_4$@NaGd$_{0.785}$Tm$_{0.015}$Yb$_{0.20}$@NaYF$_4$ (15 mol% Tb). Figure S5b, reveals spheroidal-shaped nanoparticle with average size of 15.24 ± 0.05 nm and the shell layer with thickness of 2.9 ± 0.2 nm.

Supplementary note S5 – UC properties of core@shell@shell nanoparticles
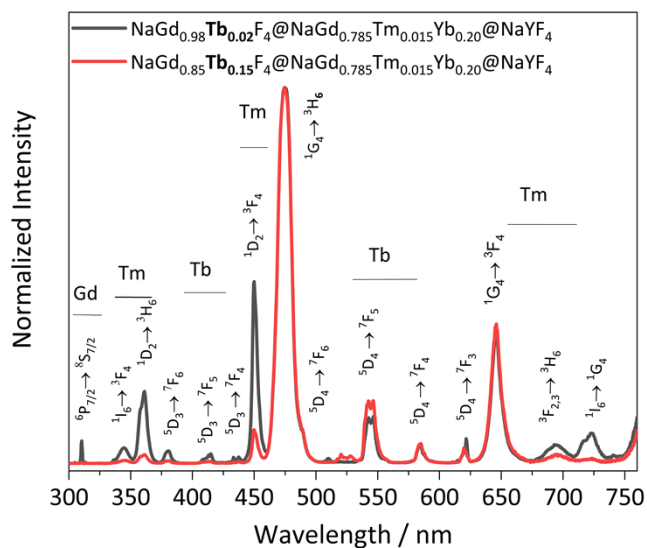
**Figure S7.** Upconversion spectra (298 K) of β- $NaGd_{0.98}\mathbf{Tb_{0.02}}F_4@NaGd_{0.785}Tm_{0.015}Yb_{0.20}F_4@NaYF_4$ (2 mol% Tb) and β- $NaGd_{0.85}\mathbf{Tb_{0.15}}F_4@NaGd_{0.785}Tm_{0.015}Yb_{0.20}F_4@NaYF_4$ (15 mol% Tb) powder nanoparticles upon 980 nm excitation.
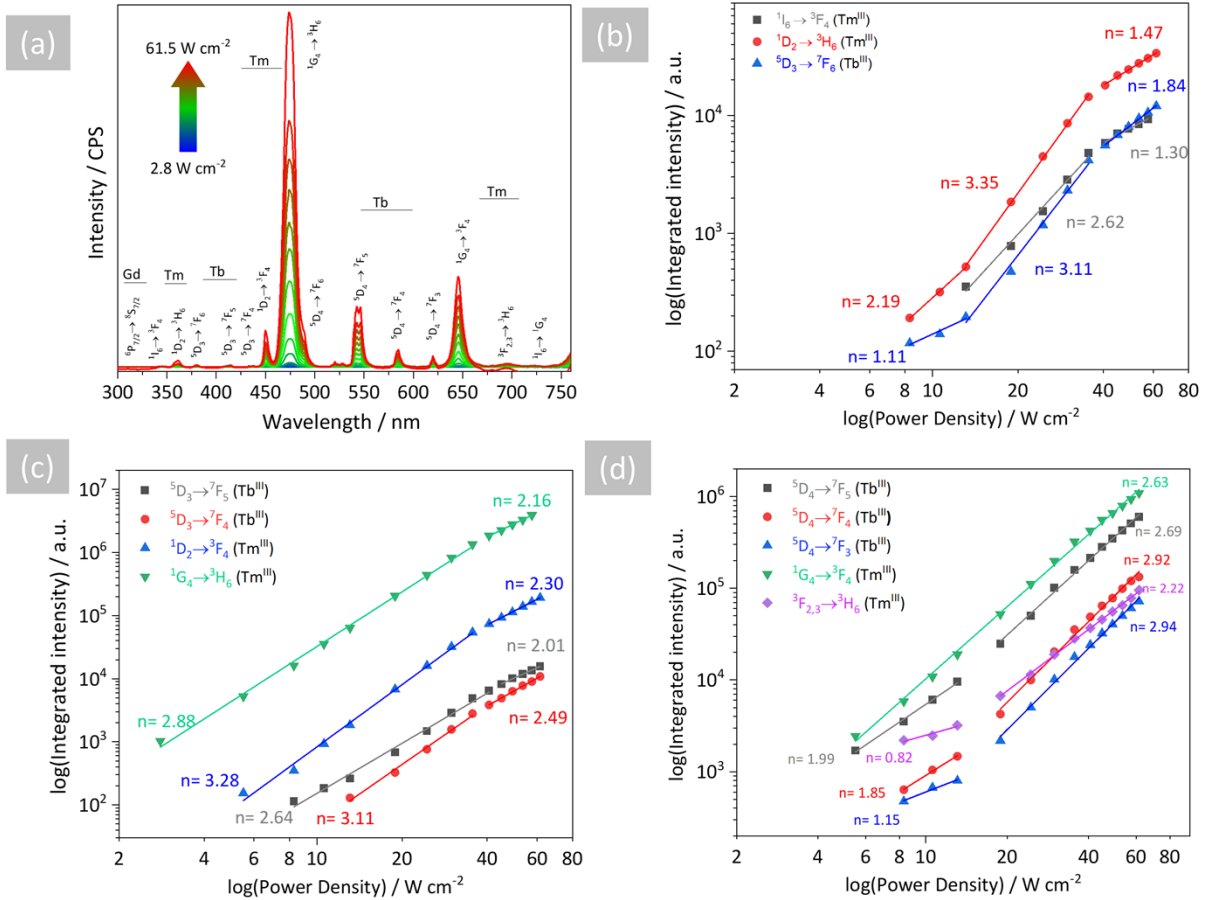
Figure S8. (a) Upconversion spectra (298 K) at P_{exc} ranging from 2.8 to 61.5 W cm^{-2} under 980 nm excitation. Dependence of integrated intensities versus P_{exc} considering (b) 300 to 400 nm, (c) 400 to 500 nm, and (d) 500 to 760 nm spectral region of β-NaGd$_{0.765}$**Tb$_{0.15}$**F$_4$@NaGd$_{0.785}$Tm$_{0.015}$Yb$_{0.20}$F$_4$@NaYF$_4$ (15 mol% Tb) powder nanoparticles.

Supplementary note S6 – DS and DC characterization of core@shell@shell nanoparticles
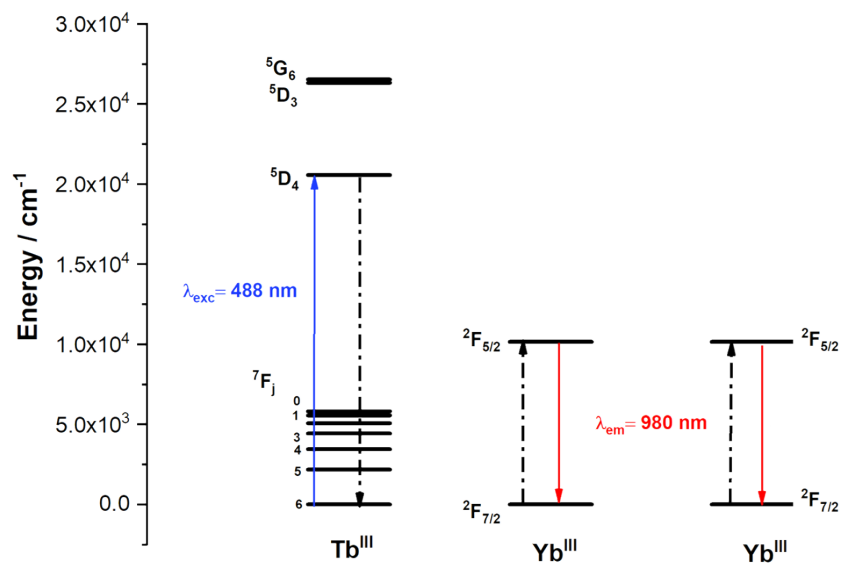

Figure S9. Schematic energy level diagram showing the proposed energy transfer mechanism of the quantum-cutting process, involving one photon, under 488 nm laser excitation.
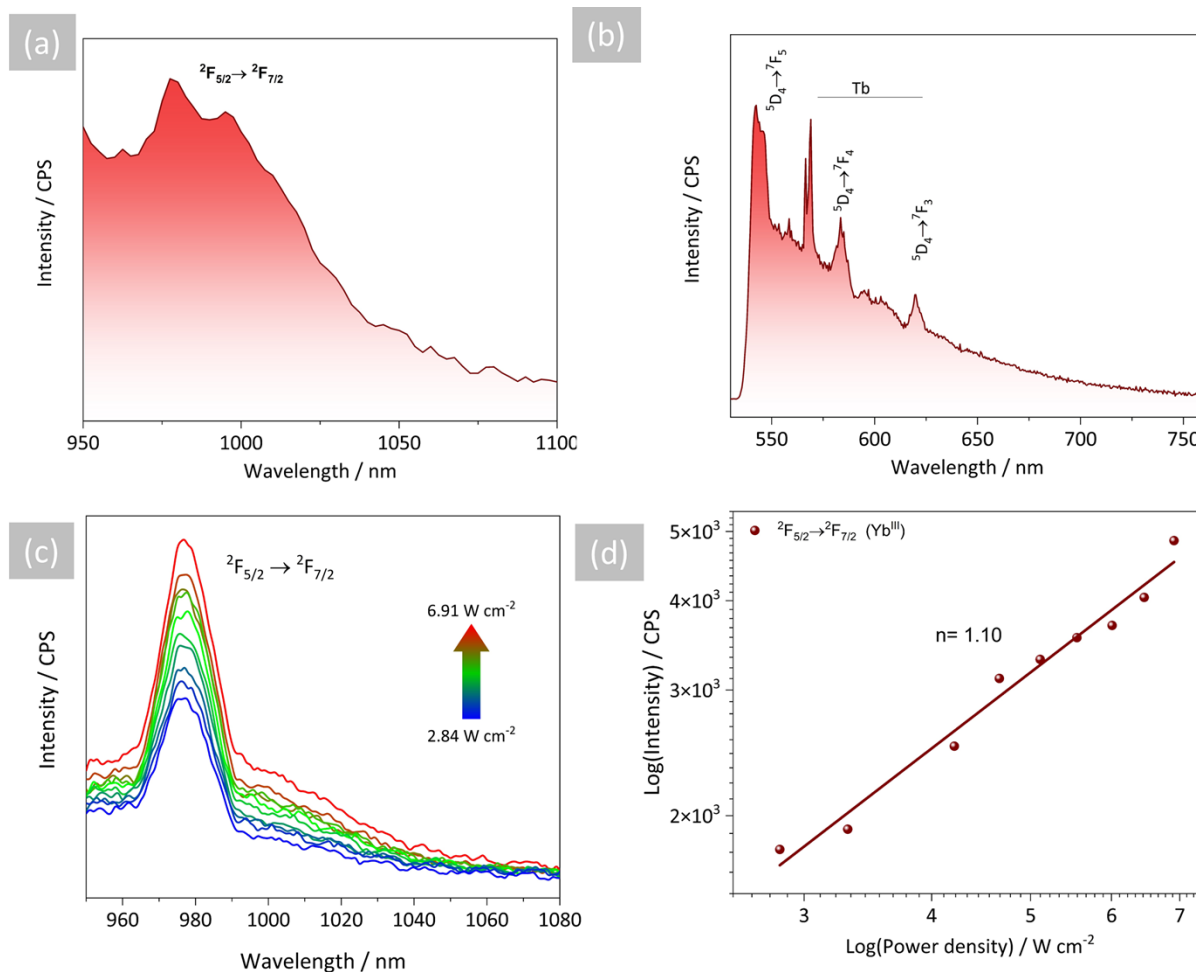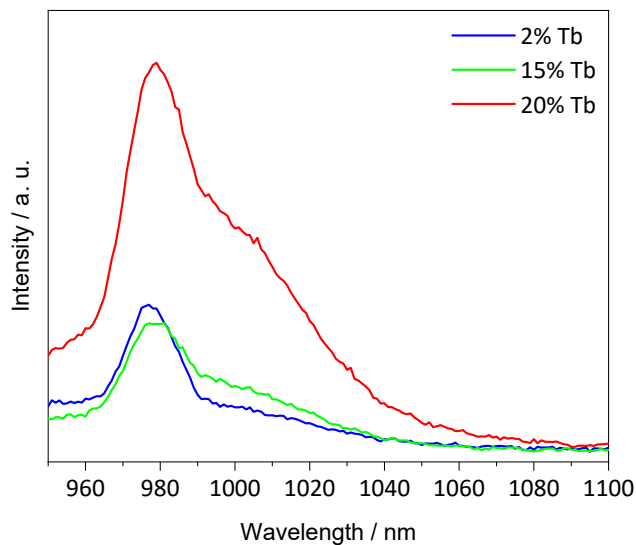
Figure S10. (a) Emission spectrum (λ_{exc}= 488 nm) of powder nanoparticles. (b) Emission spectrum in the visible region under laser excitation at 488 nm. (c) Quantum-cutting spectra at P_{exc} 2.84 to 6.91 W cm^{-2} under 488 nm laser excitation. (d) Dependence of integrated intensities versus excitation optical power of β- NaGd$_{0.98}$**Tb$_{0.02}$**F$_4$@NaGd$_{0.785}$Tm$_{0.015}$Yb$_{0.20}$F$_4$@NaYF$_4$ (2 mol% Tb) nanoparticles dispersed in cyclohexane (30 mg mL^{-1}).
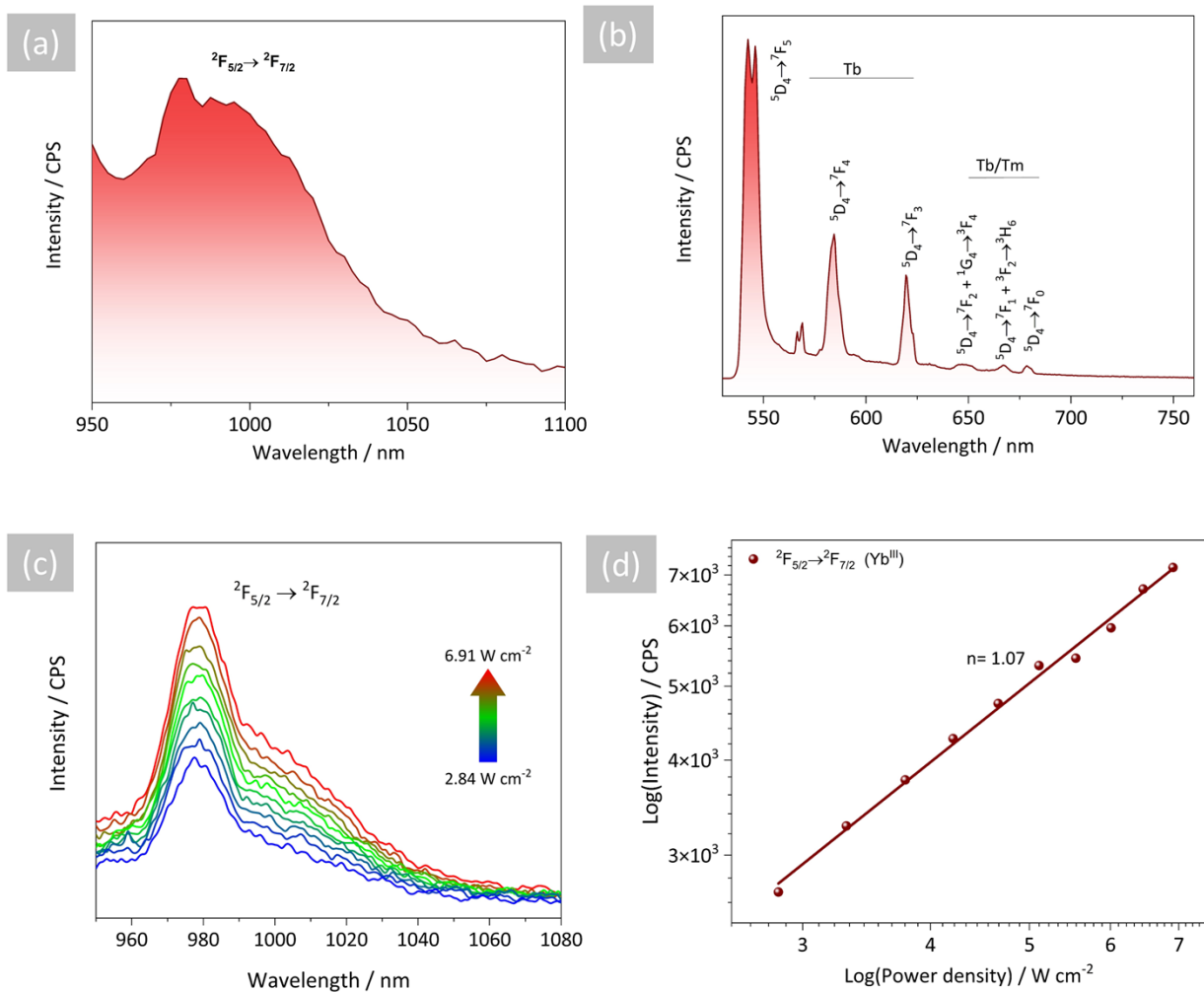
Figure S11. (a) Emission spectrum (λ_{exc}= 488 nm) of powder nanoparticles. (b) Emission spectrum in the visible region under laser excitation at 488 nm. (c) Quantum-cutting spectra at P_{exc} ranging from 2.84 to 6.91 W cm^{-2} under 488 nm laser excitation. (d) Dependence of integrated intensities versus excitation optical power of β- NaGd$_{0.85}$**Tb$_{0.15}$**F$_4$@NaGd$_{0.785}$Tm$_{0.015}$Yb$_{0.20}$F$_4$@NaYF$_4$ (15 mol% Tb) nanoparticles dispersed in cyclohexane (30 mg mL^{-1}).
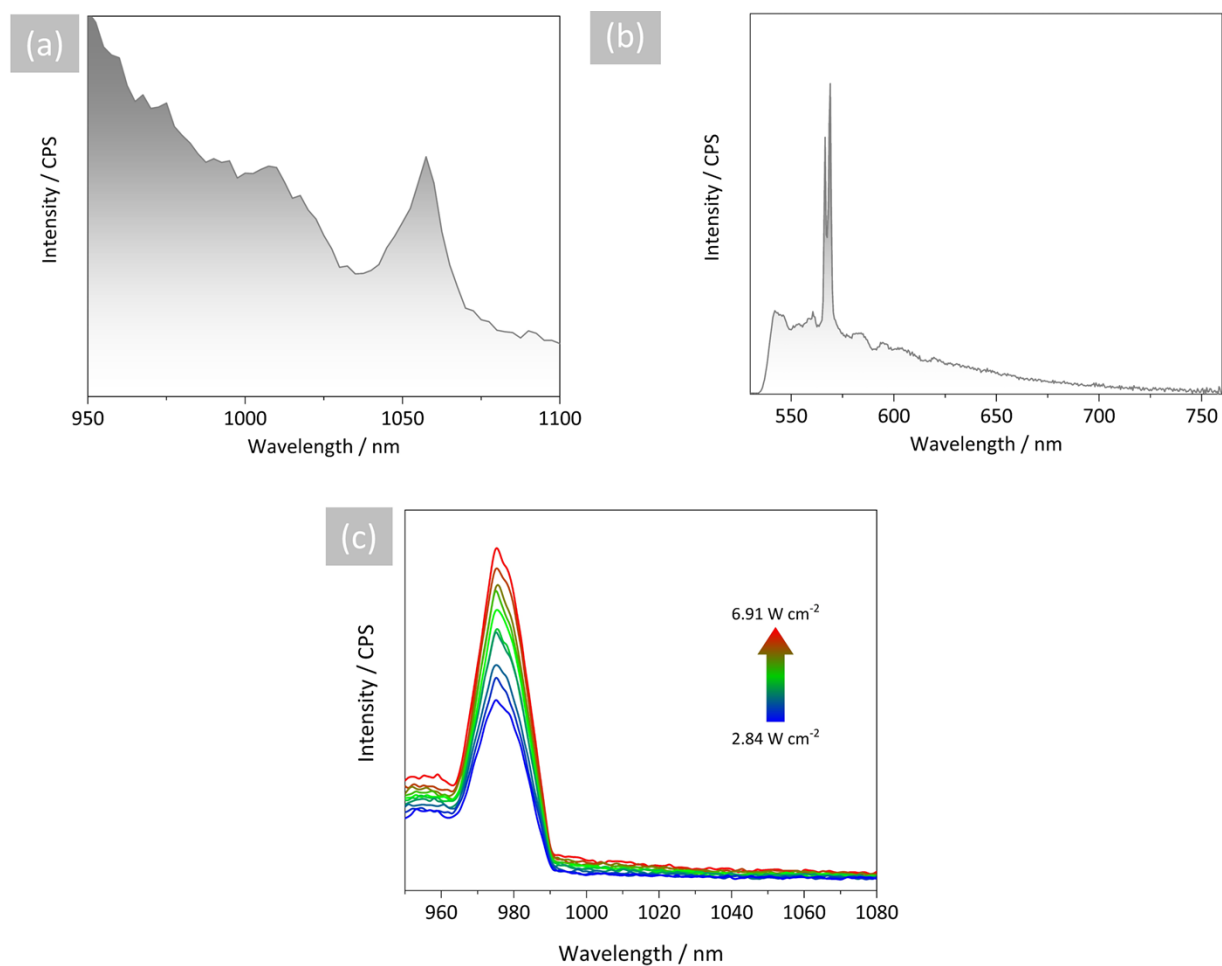
Figure S12. (a) Emission spectrum (λ_{exc}= 488 nm) of powder nanoparticles. (b) Emission spectrum within the visible region under laser excitation at 488 nm. (c) Quantum-cutting spectra at P_{exc} ranging from 2.84 to 6.91 W cm^{-2} under 488 nm laser excitation of β-NaGdF$_4$@NaYF$_4$ nanoparticles dispersed in cyclohexane (30 mg mL^{-1}).

Figure S13. Emission spectrum (λ_{exc}= 488 nm, P_{exc} = 9.61 W cm^{-2}) of NaGd$_{y-x}$**Tb$_x$**F$_4$@NaGd$_{0.785}$Tm$_{0.015}$Yb$_{0.20}$F$_4$@NaYF$_4$ with different Tb^{III} doping amounts.

Supplementary references

[1] E. M Rodrigues, D. A. Gálico, M. A. Lemes, J. Bettini, E. T. Neto, I. O. Mazali, M. Murugesu, F. A. Sigoli, *New J. Chem.* 2018, **42**, 13393.

[2] C. M. S. Calado, Í. F. Manali, I. M. S. Diogenis, S. F. N. Coelho, V. C. Texeira, B. R.de Mesquita, J. L. Oliveira, F. A. Sigoli, M.V. dos S. Rezende. *Opt. Mater.* 2023, **137**, 113529.

[3] I. M. S. Diogenis, E. M. Rodrigues, I. O Mazali, F. A. Sigoli, *J. Lumin.* 2021, **232**, 117848.

[4] F. S. Ferreira, A. J. de Morais, C. M. S. Calado, F. Iikawa, O. D. D. Couto Junior, G. Brunet, M. Murugesu, I. O. Mazali, F. A. Sigoli, Nanoscale, 2021, **13**, 14723